

APPENDIX B: UPPER BOUND FOR $G_u(s, z)$ IN $|z| < 1$

In this Appendix we estimate the upper bound of $G_u(s, z)$ in $|z| < 1$. Using the inequality (48) and Eq. (23), for $|z| < 1$, we have

$$|G_u(s, z)| < s^{N_6} [1 - f_{x \ln s - 1}(s)] \sum_{l=0}^{x \ln s - 1} (2l + 1) + s^{N_6} \sum_{l=0}^{\infty} (2l + 2x \ln s + 1) |z|^{l + x \ln s}, \quad (61)$$

$$< \text{const.} (\ln^3 s) s^{N_6 - \alpha/x} + \text{const.} |z|^{x \ln s} s^{N_6} + \text{const.} z^{x \ln s} s^{N_6} \ln s. \quad (62)$$

Putting $x = [-\alpha / \ln |z|]^{1/2}$ and $|z| = 1 - \epsilon$, we obtain the inequality (26).

APPENDIX C: ANALYTICITY AND THE UPPER BOUND FOR $G_{2u}^L(s, z)$

The difference between $G_{2u}^L(s, z)$ and $G_{2u}(s, z)$ essential for this argument is the absence of the right-hand cut in $G_{2u}^L(s, z)$. By virtue of this difference, we have only $b_l'(s)$ and no term corresponding to $b_l(s)$ in Eq. (55). Therefore it is obvious that $G_{2u}^L(s, z)$ is analytic in the domain in which $|z|$ is finite and $\pi - \theta_0/n > \arg z > -\pi - \theta_0/n$. By the procedure used for the calculation of the bounds for $G_u(s, z)$ in Appendices A and B, we can obtain similar upper bounds for $G_{2u}^L(s, z)$ on C_1' and C_3' .

Overlapping Resonances in Dispersion Theory*

JOHN B. BRONZAN†

Laboratory for Nuclear Science and Department of Physics, Massachusetts Institute of Technology, Cambridge, Massachusetts

(Received 23 December 1963)

The Khuri-Treiman dispersion representation is applied to the discussion of overlapping resonances among particles in production and decay final states. The kernel of the dynamical equation following from the Khuri-Treiman representation has branch points overlapping the integration contour, but recently reported work permits us to select the correct branch of the kernel. We thus eliminate all restrictions on the masses of the final-state particles or strengths of the resonances. An iteration procedure is developed for the solution of the dynamical equation when three spinless particles are present in the final state. There is no restriction on the angular momentum of the resonances, but for simplicity only s -wave resonances are considered here. Plausibility arguments are given which indicate that for narrow resonances the once-iterated approximation to the solution is a good approximation. A detailed study of all higher approximations supports this assertion. In the once-iterated approximation, one finds a branch point on the second sheet of the transition amplitude which may cause a characteristic variation of the amplitude near the low-energy boundaries of the physical region. This variation is studied quantitatively for the kinematically favorable reaction $N+N \rightarrow N+N+\pi$, and is found to be of negligible importance. The suppression of the variation is related to the threshold behavior of two-particle scattering amplitudes.

I. INTRODUCTION

IN this paper we discuss the role of resonant final-state interactions in production and decay reactions leading to three-particle final states. In particular, we study what happens when two of the three outgoing particles are identical and either one (or both) scatters resonantly with the third. Following Peierls and Tarski,¹ we call this the case of overlapping resonances. As is well known, this class of reactions includes cases of great current interest, for instance,

$$\bar{K} + N \rightarrow Y^* + \pi \rightarrow \begin{pmatrix} \Lambda + \pi + \pi \\ \Sigma + \pi + \pi \end{pmatrix},$$

$$\pi + N \rightarrow N^* + \pi \rightarrow N + \pi + \pi,$$

$$N + N \rightarrow N^* + N \rightarrow N + N + \pi,$$

where the π - π resonances are excluded kinematically. The restrictions to two identical particles and only two resonances are made for convenience. The methods we use can be extended to study π - π resonances in the reactions above, or to study

$$\bar{K} + N \rightarrow \begin{pmatrix} \bar{K}^* + N \\ N^* + \bar{K} \end{pmatrix} \rightarrow N + \bar{K} + \pi,$$

$$\bar{N} + N \rightarrow \begin{pmatrix} \rho + \pi \\ f^0 + \pi \end{pmatrix} \rightarrow \pi + \pi + \pi.$$

The dynamics of our treatment are provided by the Khuri-Treiman² (KT) dispersion representation of a

* This work is supported in part through funds provided by the Atomic Energy Commission under Contract AT(30-1)2098. Part of a thesis submitted to Princeton University in candidacy for the degree of Doctor of Philosophy, May 1963.

† National Science Foundation Predoctoral Fellow, 1962-1963.

¹ R. F. Peierls and J. Tarski, Phys. Rev. **129**, 981 (1963).

² N. N. Khuri and S. B. Treiman, Phys. Rev. **119**, 1115 (1960).

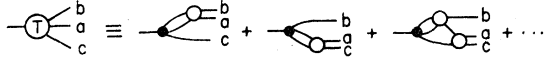


FIG. 1. Final-state scattering diagrams and their KT sum.

decay amplitude. This representation effectively sums a class of perturbation graphs which contribute to final-state scattering, but it excludes graphs which give rise to complex thresholds, and make the “analyticity and unitarity” treatment of production and decay amplitudes so difficult.³ We want to emphasize that here dispersion theory performs much more than its usual service of relating one strong interaction process to others. The process at hand is a three-body process, and any conventional treatment would almost certainly be very difficult. We have no deep understanding of why dispersion theory is such a powerful tool here, but simply point out that it is.

The dynamical integral equation which follows from the KT representation reflects the three-body complications by the presence of a kernel with branch points which overlap the interval of integration. In previous discussions the problem of determining the physical branch of the kernel has been bypassed, either by assuming that the final-state interactions are weak,² or by doing away with three-body kinematics by going to a static limit,¹ or by an approximation which simplifies the analytic structure of the kernel.⁴ In the present paper we make use of a recent analysis by Bronzan and Kacser⁵ to obtain the physical branch of the kernel. The restriction to resonant final-state interactions is made after the dynamical equation, valid for any interaction, is obtained. Our motivation for the restriction is that final-state interactions play a most conspicuous role when they are resonant.

In Sec. II we write down the KT dispersion relation and obtain the dynamical integral equation. The general properties of this equation are discussed, and the iteration procedure of solution is developed. In Sec. III the once-iterated solution is presented. A logarithmic branch point is found which is on the second Riemann sheet of the transition amplitude, but is so close to the physical edge of the physical sheet that it may have observable consequences. The same branch point has been discussed in perturbation theory by Aitchison.⁶ The location and presence of the branch point are interpreted physically. Singularities present in all further iterations are located and found to be less important than the branch point in the first iteration. In Sec. IV the significance of the branch point is investigated in a specific case. It is found that it produces no visible structure in the square of the transition amplitude. The reason for this disagreement with Aitchison is linked to unitarity requirements.

³ See P. V. Landshoff and S. B. Treiman, *Nuovo Cimento* **19**, 1249 (1961) for examples of complex thresholds.

⁴ D. R. Harrington, *Phys. Rev.* **130**, 2502 (1963).

⁵ J. B. Bronzan and C. Kacser, *Phys. Rev.* **132**, 2703 (1963).

⁶ I. J. R. Aitchison, *Phys. Rev.* **133**, B1257 (1964).

II. THE DYNAMICAL EQUATION AND ITS PROPERTIES

We consider the influence of final-state scattering on reactions leading to the production of spinless particles a , b , and c . To be specific, we study the decay of a particle of mass M into a , b , and c , and assume that such a decay represents a reasonable model for the study of final-state scattering in production reactions as well. For convenience, we assume b and c are identical particles of mass μ , while a has mass m . The generalization to three different masses is straightforward, but leads to no new insight. Also for simplicity, we assume b and c scatter resonantly with a , but do not interact with each other.

In the production reaction case, M is the energy of the colliding system, and is a parameter at our disposal. Since the unstable particle is spinless, our model pertains only to production in s waves, and we forgo any description of the dependence of the transition amplitude T on momentum transfers between incoming and outgoing particles. In addition to M and two independent momentum transfers, a production reaction depends upon three variables which specify the configuration of final-state momenta. These are

$$s_a = (p_M - p_a)^2, \quad s_b = (p_M - p_b)^2, \quad s_c = (p_M - p_c)^2, \quad (2.1)$$

$$p_M^2 = M^2, \quad p_a^2 = m^2, \quad p_b^2 = p_c^2 = \mu^2.$$

These variables are not independent, but satisfy the equation

$$s_a + s_b + s_c = M^2 + m^2 + 2\mu^2. \quad (2.2)$$

As was mentioned in the Introduction, it is easy to find perturbation diagrams which give rise to complex thresholds of the transition amplitude $T(s_a, s_b, s_c)$.^{3,7} But there exists a class of diagrams, illustrated in Fig. 1, which have only normal thresholds. The sum of the amplitudes of this class satisfies the KT dispersion representation

$$T(s_a, s_b, s_c) = \frac{1}{\pi} \int_{(m+\mu)^2}^{\infty} \frac{ds'_b \Phi(s'_b, s_c)}{s'_b - s_b - i\epsilon}$$

$$+ \frac{1}{\pi} \int_{(m+\mu)^2}^{\infty} \frac{ds'_c \Phi(s'_c, s_b)}{s'_c - s_c - i\epsilon}, \quad (2.3)$$

where the spectral function is

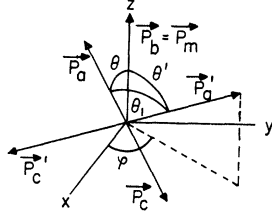
$$\Phi(s_b, s_c) = \frac{(2\pi)^4}{2} [4p_M^0 p_c^0]^{1/2} \sum_n \langle p_c | f(0) | n \rangle$$

$$\times \langle n | j(0) | p_M \rangle \delta(p_n - p_M + p_b). \quad (2.4)$$

Here $j(0)(f(0))$ is the current operator for the source of the $\mu(m)$ field. We include only two-particle intermediate states in the summation (2.4), since in our

⁷ See G. Barton and C. Kacser, *Nuovo Cimento* **21**, 988 (1961) for another example.

FIG. 2. Momenta in the Lorentz frame $\mathbf{p}_a + \mathbf{p}_c = 0$. \mathbf{p}_a is in the x - z plane with $p_{ax} > 0$.



model final-state scattering is supposed to play a dominant role. It is in the spirit of the model to omit Born terms as well as three or more particle intermediate states. We note that

$$\begin{aligned} \langle p_a' p_c' \text{ out} | j(0) | p_M \rangle &= [8p_{M0} p_{a0}' p_{c0}']^{-1/2} T(s_a', s_b, s_c'), \\ \langle p_c | f(0) | p_a' p_c' \text{ out} \rangle &= 4\pi (p_{a0}' + p_{c0}') [2p_{c0} p_{a0}' p_{c0}']^{-1/2} f^*, \end{aligned} \quad (2.5)$$

where f is the scattering amplitude for the process $p_a + p_c \rightarrow p_a' + p_c'$.

To evaluate Φ we go to the Lorentz frame $\mathbf{p}_a + \mathbf{p}_c = 0$. (See Fig. 2.) In this frame, $p = |\mathbf{p}_M| = |\mathbf{p}_b|$, $k = |\mathbf{p}_a| = |\mathbf{p}_c| = |\mathbf{p}_a'| = |\mathbf{p}_c'|$. We define the variables

$$\begin{aligned} s_b &= (p_M - p_b)^2 = ([p^2 + M^2]^{1/2} - [p^2 + \mu^2]^{1/2})^2 \\ &= ([k^2 + m^2]^{1/2} + [k^2 + \mu^2]^{1/2})^2, \\ s_c &= (p_M - p_c)^2 = -p^2 - k^2 - 2pk \cos\theta \\ &\quad + ([p^2 + M^2]^{1/2} - [k^2 + \mu^2]^{1/2})^2, \\ s_c' &= (p_M - p_c')^2 = -p^2 - k^2 - 2pk \cos\theta' \\ &\quad + ([p^2 + M^2]^{1/2} - [k^2 + \mu^2]^{1/2})^2. \end{aligned} \quad (2.6)$$

We can now express $\cos\theta$ in terms of s_b and s_c .

$$\begin{aligned} \cos\theta &\equiv \cos\theta_b(s_c) = R(s_b, s_c) / [U(s_b)]^{1/2}, \\ R(s_b, s_c) &= -s_b^2 + (M^2 + m^2 + 2\mu^2 - 2s_c)s_b \\ &\quad + (M^2 - \mu^2)(m^2 - \mu^2), \\ U(s_b) &= [s_b - (m - \mu)^2][s_b - (m + \mu)^2] \\ &\quad \times [s_b - (M - \mu)^2][s_b - (M + \mu)^2]. \end{aligned} \quad (2.7)$$

In (2.7), $\cos\theta_b(s_c)$ is the angle between \mathbf{p}_a and \mathbf{p}_b in the Lorentz frame $\mathbf{p}_a + \mathbf{p}_c = 0$, and s_c indicates the variable which $\theta_b(s_c)$ replaces. Thus $\cos\theta' = \cos\theta_b(s_c')$. We note that $[U(s_b)]^{1/2} = 4kps_b > 0$ in the physical decay interval $(m + \mu)^2 \leq s_b \leq (M - \mu)^2$.

In the b frame (2.4) becomes

$$\begin{aligned} \Phi(s_b, s_c) &= \frac{1}{4\pi} \int k'^2 dk' d\theta' d\varphi \delta(p_{a0}' + p_{c0}' - p_{a0} - p_{c0}) \\ &\quad \times \frac{p_{a0}' + p_{c0}'}{p_{a0}' p_{c0}'} T(s_a', s_b, s_c') f^*(s_b, \cos\theta_1). \end{aligned} \quad (2.8)$$

For f we use the angular momentum decomposition

$$f(s, \cos\theta_1) = \sum_{l=0}^{\infty} (2l+1) f_l(s) P_l(\cos\theta_1). \quad (2.9)$$

It is convenient to assume that scattering is important quantitatively in only one partial wave. For simplicity we take this partial wave to be the s wave.⁸ Then we obtain a spectral function which depends on only one variable.

$$\begin{aligned} \Phi(s_b) &= f_0^*(s_b) T_0(s_b), \\ T_0(s_b) &= \frac{1}{2} \int_{-1}^1 d \cos\theta_b(s_c') T(s_a', s_b, s_c'). \end{aligned} \quad (2.10)$$

Here $T_0(s_b)$ is the s -wave projection of T in the frame $\mathbf{p}_a + \mathbf{p}_c = 0$. (2.3) and (2.10) constitute the KT dispersion representation. We obtain an integral equation for $T_0(s)$ by operating on (2.3) with the s -wave projection operator. The result is

$$\begin{aligned} T_0(s) &= \frac{1}{\pi} \int_{(m+\mu)^2}^{\infty} ds' f_0^*(s') T_0(s') \\ &\quad \times \left\{ \frac{1}{s' - s - i\epsilon} + G(s, s' - i\epsilon, M^2) \right\}, \end{aligned} \quad (2.11)$$

where

$$G(s_b, s_c' - i\epsilon, M^2) = \frac{1}{2} \int_{-1}^1 d \cos\theta_b(s_c) \frac{1}{s_c' - s_c - i\epsilon}. \quad (2.12)$$

Substituting from (2.7) for s_c ,

$$\begin{aligned} G(s_b, s_c' - i\epsilon, M^2) &= \frac{s_b}{[U(s_b)]^{1/2}} \int_{-1}^1 dx \left\{ x - \frac{R(s_b, s_c' - i\epsilon)}{[U(s_b)]^{1/2}} \right\} \\ &= -\frac{s_b}{[U(s_b)]^{1/2}} \ln \frac{R(s_b, s_c' - i\epsilon) + [U(s_b)]^{1/2}}{R(s_b, s_c' - i\epsilon) - [U(s_b)]^{1/2}}. \end{aligned} \quad (2.13)$$

Equations (2.11) and (2.13) define our dynamical model for studying overlapping final-state interactions. We can see at this point what is surprising about the dispersion theoretic treatment. As expected, we get the transition amplitude T as a functional of the two-body scattering amplitude $f_0(s)$, but the equation we obtain, (2.11), depends on only one scalar variable.

In order that (2.11) be a well-defined equation, we must know G throughout the quadrant $(m + \mu)^2 \leq s, s' < \infty$. On the other hand, in performing the unitarity sum (2.4), we were confined to the physical region bounded by $R(s, s') / [U(s)]^{1/2} = \pm 1$, which lies in one corner of the quadrant. (See Fig. 4.) The kernel must be obtained throughout the rest of the quadrant by analytic continuation in s and s' . This has been done in Ref. 5, and the analysis carried out there can be applied directly to (2.11). We repeat here only the main conclusions of Ref. 5.

⁸ The essential results of this paper have been carried out for arbitrary angular momentum, J. B. Bronzan, Princeton University thesis (unpublished). The conclusions we present are unaffected by the value of l .

There are two types of singularities of (2.13) to consider: The endpoint singularities $R(s,s')/[U(s)]^{1/2} = \pm 1$, and the branch points of $[U(s)]^{1/2}$. The curves of possible singularity are thus the boundary of the physical region, which for a decay amplitude lies in the critical quadrant, and the kinematic or non-Landau singularities of $[U(s)]^{1/2}$. In Sec. 2 of Ref. 5 it was found that with the boundary prescription given to us by KT, $G(s, s'-i\epsilon, M^2)$ has a branch point at $s = (M+\mu)^2$ for $(m+\mu)^2 \leq s' \leq M\mu + (Mm^2 - \mu^3)/(M-\mu)$. It was observed that simply giving s' a negative imaginary part is not sufficient to prescribe how to pass this branch point, whose location is independent of s' . The problem was attacked by analyzing the diagram shown in Fig. 3 in perturbation theory. This diagram is one of the diagrams which contributes to the KT sum. Its transition amplitude, which for point vertices is identical to the s -wave projection of its transition amplitude, has a dispersion representation with $G(s,s',M^2)$ appearing in its spectral function. As always, perturbation theory gives an unambiguous specification of the physical sheet of $G(s,s',M^2)$, although in this case some care is required to extract the specification.

There are several equivalent ways of stating the implications of perturbation theory. The most concise is to say that on its physical sheet $G(s,s',M^2)$ is real for $s, s' > (M+\mu)^2$, and for smaller s and s' one continues in these variables, in either order, but letting $M^2 \rightarrow M^2 + i\delta$ rather than $s' \rightarrow s' - i\epsilon$ to get the physical sheet of G . This does not mean that there is a contradiction between KT and perturbation theory. In the first place, the negative imaginary part of s' comes from (2.3), where it specifies the physical branch of T . Hence, it must be present. However, we find that in taking the s -wave projection of T , (2.11), one must also let M^2 have a positive imaginary part which overrides the imaginary part of s' . We must consider $T(s_a, s_b, s_c, M^2)$ to be a function of the complex variable M^2 , with the physical decay amplitude defined by

$$T(s_a, s_b, s_c, M^2) = \lim_{\delta \rightarrow 0} \lim_{\epsilon \rightarrow 0} T(s_a, s_b - i\epsilon, s_c - i\epsilon, M^2 + i\delta). \quad (2.14)$$

The crucial point is that the limits are taken in the order shown. Of course, Khuri and Treiman had no way of knowing about the M^2 prescription. We point out that it is only because the branch points of G overlap the critical quadrant that the order of taking limits becomes a sensitive matter.

We can now give the physical branch of G explicitly. When M^2 has a positive imaginary part, the bothersome branch points of $[U(s)]^{1/2}$ at $(M+\mu)^2$ move into the upper half s plane. From (2.13), once the imaginary



FIG. 3. Perturbation diagram studied by Bronzan and Kacser.

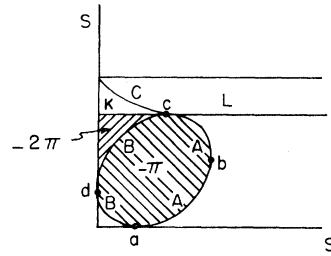


FIG. 4. The imaginary part of the logarithm in (2.13) on the physical branch of $G(s, s', M^2 + i\delta)$. On Curve A, $R(s, s') + [U(s)]^{1/2} = 0$, and the numerator of the logarithm vanishes. On the curve B, $R(s, s') - [U(s)]^{1/2} = 0$, and the denominator vanishes. Together A and B bound the physical region. C is a segment of the curve $R(s, s') = 0$. The imaginary part in region K is between $-\pi$ and -2π , while in region L it is between 0 and $-\pi$. In the shaded regions the imaginary part is the indicated constant, and elsewhere it is zero. The points a, b, c and d are:

a	$(m+\mu)^2$	$-m\mu + (M^2m + \mu^3)/(m+\mu)$
b	$M\mu + (Mm^2 - \mu^3)/(M-\mu)$	$(M-\mu)^2$
c	$(M-\mu)^2$	$M\mu + (Mm^2 - \mu^3)/(M-\mu)$
d	$-m\mu + (M^2m + \mu^3)/(m+\mu)$	$(m+\mu)^2$

part of the logarithm is given, the branch of G is defined; and the imaginary part of the logarithm is shown in Fig. 4. In Fig. 5 we show the trajectory of the singularities at

$$\frac{R(s,s')}{[U(s)]^{1/2}} = \pm 1, \quad s = s_{\pm}(s') = \frac{1}{2s'} \{R(s',0) \pm [U(s')]^{1/2}\}, \quad (2.15)$$

as s' moves along the arc $(m+\mu)^2 \leq s' < \infty$. This shows the overlap explicitly.

There are two general observations to be made about $T_0(s)$. First, it has a singularity at $s = (M-\mu)^2 + i\delta$. This arises because the logarithm has a nonvanishing imaginary part at $s = (M-\mu)^2$ for $(m+\mu)^2 \leq s' < M\mu + (Mm^2 - \mu^3)/(M-\mu)$. This branch point replaces the branch point we initially found at $s = (M+\mu)^2$ when we followed the boundary prescription $s' - i\epsilon$ for G . It causes $T(s_a, s_b, s_c)$ to be singular at $s_b = (M-\mu)^2$ and $s_c = (M-\mu)^2$, but on the unphysical boundary of the physical sheet. On the physical boundary, T is of course analytic at $s_b, s_c = (M-\mu)^2$.

The second observation is that in general $T_0(s)$ has a branch point at $s = -m\mu + (M^2m + \mu^3)/(m+\mu) + i\delta$. This is an endpoint singularity located at point d in Figs. 4 and 5. Again, T has singularities only on the unphysical boundary of the physical sheet.

The singularities of T_0 just mentioned are kinematical, and follow from the vanishing of momenta. To make further progress one must specify the scattering amplitude $f_0(s)$. We parametrize $f_0(s)$ by the Breit-Wigner amplitude

$$f_0(s) = \frac{-\Gamma[s - (M+\mu)^2]^{1/2}}{s - s_0 + i\Gamma[s - (m+\mu)^2]^{1/2}}, \quad (2.16)$$

which has a resonance at s_0 , behaves like an s -wave amplitude at threshold, has its resonance pole in the lower half plane (so that it corresponds to a decaying state), and satisfies elastic unitarity,

$$\text{Im}f_0(s) = |f_0(s)|^2. \tag{2.17}$$

In terms of $s^{1/2}$, the invariant mass, the full width of the resonance at half-maximum is

$$\gamma = \frac{\Gamma[s_0 - (m + \mu)^2]^{1/2}}{s_0^{1/2}}. \tag{2.18}$$

Thus, we replace the arbitrary scattering amplitude $f_0(s)$ by two parameters, s_0 and Γ , which remain at our disposal. If Γ is small the resonance in $f_0(s)$ is very narrow. Physically this means that the isobar formed between m and μ is long lived on the time scale of strong processes, so that m is quite distant from the non-resonant μ when the isobar decays. In this limit the overlapping interaction must be unimportant dynamically, although Bose symmetrization requires the resonance to appear in both the s_b and s_c spectra; that is, as two bands. The symmetrization is performed automatically by the KT representation (2.3).

We expect the dynamical effect of the overlapping resonance to become large as Γ is increased. We estimate that its effect will be comparable to that of the primary resonance when the lifetime of the resonant state, as given by the uncertainty principle, is equal to the time it takes light to cross the meson cloud of m or μ . This cloud contains pions as its lightest constituent, so the overlapping resonance has a large effect by the time $\gamma \sim 150$ MeV. For resonances narrow compared to 150 MeV, these observations suggest an approximation scheme for the solution of (2.11). The dynamical effect of the overlapping resonance is given by the term with kernel G . As a first approximation we solve the integral equation with this "overlapping" term omitted. The first approximation is thus the exact solution of the problem where final-state scattering occurs between only one pair of final-state particles. If we write $T_{0,i}(s)$ for the i th approximation to $T_0(s)$, then our approximation scheme is given by

$$\begin{aligned} T_{0,0}(s) &= \frac{1}{\pi} \int_{(m+\mu)^2}^{\infty} \frac{ds' f_0^*(s') T_{0,0}(s')}{s' - s - i\epsilon}, \\ T_{0,i+1}(s) &= \frac{1}{\pi} \int_{(m+\mu)^2}^{\infty} \frac{ds' f_0^*(s') T_{0,i}(s')}{s' - s - i\epsilon} \\ &\quad + \frac{1}{\pi} \int_{(m+\mu)^2}^{\infty} ds' f_0^*(s') \\ &\quad \times G(s, s', M^2 + i\delta) T_{0,i}(s'). \end{aligned} \tag{2.19}$$

If this sequence converges, its limit is $T_0(s)$. Actually, the question of the existence and uniqueness of solutions

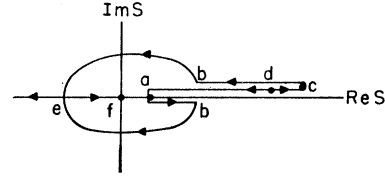


FIG. 5. Trajectories of the singularities $R(s, s') \pm [U(s)]^{1/2} = 0$ in the complex s plane as s' moves from $(m + \mu)^2$ to ∞ . M^2 has a small positive imaginary part. The points are identified in Fig. 4, except e : $s = -M\mu + (Mm^2 + \mu^2)/(M + \mu)$, $s' = (M + \mu)^2$, and f : $s = 0$, $s' = \infty$.

of (2.11) has not been studied in detail. Following Omnés,⁹ we may eliminate the Cauchy singularity from (2.11), converting the integral equation into a Fredholm-type equation. By a change of variables, the domain of the kernel can be made finite. Then, for M^2 having a finite positive imaginary part, the kernel is square integrable, and classical Fredholm theory applies. An arbitrary entire function appears in the process of converting to a Fredholm equation, but apart from this the Fredholm equation will in general have just one solution. However, the Fredholm kernel will not be square integrable when M^2 becomes real because of the non-Landau singularity of $G(s, s', M^2)$ at $s = (M - \mu)^2$. We have not followed through the consequences of this observation, but instead assume that a solution of (2.11) exists, and on the physical grounds indicated above that our iteration procedure gives a good approximation to the solution.

III. THE APPROXIMATE SOLUTION AND ITS INTERPRETATION

The equation for $T_{0,0}(s)$ is of the Omnés type,⁹ and up to a multiplicative entire function, which we take to be a constant,

$$\begin{aligned} T_{00}(s) &= \exp u(s), \\ u(s) &= -\frac{[s - (m + \mu)^2]}{2\pi i} \\ &\quad \times \int_{(m+\mu)^2}^{\infty} \frac{ds' \ln[1 - 2if_0^*(s')]}{[s' - s - i\epsilon][s' - (m + \mu)^2]}. \end{aligned} \tag{3.1}$$

Substituting from (2.16),

$$\begin{aligned} u(s) &= -\frac{[s - (m + \mu)^2]}{\pi} \int_{(m+\mu)^2}^{\infty} \frac{ds'}{[s' - s - i\epsilon][s' - (m + \mu)^2]} \\ &\quad \times \tan^{-1} \frac{\Gamma[s' - (m + \mu)^2]^{1/2}}{s' - s_0}. \end{aligned} \tag{3.2}$$

This integral is evaluated in the Appendix, and

$$T_{0,0}(s) = \frac{1}{s - s_0 + i\Gamma[s - (m + \mu)^2]^{1/2}}. \tag{3.3}$$

⁹ R. Omnés, Nuovo Cimento **18**, 316 (1958).

We point out that the manipulations above “predict” that two-body scattering resonances will appear in multiparticle final states as bumps in mass distributions when only the two particles in question interact strongly.

For $T_{0,1}$ we have

$$T_{0,1}(s) = T_{0,0}(s) + W(s),$$

$$W(s) = \frac{\Gamma s}{\pi [U(s)]^{1/2}} \int_{(m+\mu)^2}^{\infty} \frac{ds' [s' - (m+\mu)^2]^{1/2}}{(s' - s_0)^2 + \Gamma^2 [s - (m+\mu)^2]} \times \ln \frac{R(s, s') + [U(s)]^{1/2}}{R(s, s') - [U(s)]^{1/2}}. \quad (3.4)$$

$W(s)$ is computed exactly in the Appendix. However, it is in the spirit of our approximation to keep only the leading part for small Γ , which is

$$W(s) = \frac{\Gamma s}{[U(s)]^{1/2}} \ln \frac{R(s, s_0) + [U(s)]^{1/2} + iC_N(s)}{R(s, s_0) - [U(s)]^{1/2} + iC_D(s)}, \quad (3.5)$$

where

$$C_{N,D}(s) = 2s\Gamma \left\{ \frac{R(s, (m+\mu)^2) \pm [U(s)]^{1/2}}{2s} \right\}^{1/2}, \quad (3.6)$$

where N and D are given by the plus and minus signs, respectively.

The function of $C_{N,D}(s)$ is to remove the branch points of the logarithm from the real s axis. We need retain these small terms only near the branch points of the logarithm, and for s_0 in the physical interval, the branch points also lie in the physical interval, $(m+\mu)^2 \leq s \leq (M-\mu)^2$. In this interval, $C_N(s) > 0$. On the other hand, the argument of the square root for $C_D(s)$ is only positive semidefinite. It vanishes at $s = -m\mu + (M^2m + \mu^3)/(M + \mu)$, and the proper branch of $C_D(s)$ is

$$C_D(s) > 0, \quad (m+\mu)^2 \leq s < -m\mu + (M^2m + \mu^3)/(m+\mu), \quad (3.7)$$

$$< 0, \quad -m\mu + (M^2m + \mu^3)/(m+\mu) < s \leq (M-\mu)^2.$$

In order to specify the branch of $W(s)$ completely, we note that the logarithm vanishes when $s = (m+\mu)^2$.

To locate the logarithmic branch points of $W(s)$ to lowest order in Γ , we use

$$s = \bar{s}_{\pm}(s_0) = s_{\pm}(s_0) - i \frac{C(s_{\pm}(s_0))}{2s_{\pm}(s_0)} \frac{\partial}{\partial s_0} s_{\pm}(s_0), \quad (3.8)$$

where $s_{\pm}(s_0)$ is defined in (2.15). For s_0 in the physical interval, the second term is crucial and gives the imaginary coordinate of the branch point. Referring to Fig. 4, let s_0 take the place of s' . Then by inspection the derivative in (3.8) is positive on arc (ab) of curve A

and arc (cd) of B, and negative on arc (bc) of A and arc (ad) of B. On curve A, the function C in (3.8) is C_N , while on curve B, C stands for C_D . When these observations are assembled, it turns out that the branch points of $W(s)$ are in the upper half s plane, except on arc (ab) of curve A. That is, for $-m\mu + (M^2m + \mu^3)/(m+\mu) < s_0 < (M-\mu)^2$, $s_{-}(s_0)$ is in the lower half s plane.

The physical significance of this branch point becomes clear when $T_0(s)$ is substituted into (2.10) to obtain the spectral function. This spectral function is substituted into (2.3) to obtain the transition amplitude. Any singularity of $\Phi(s')$ just below the s' axis will be almost pinched by the dispersion denominator. Such singularities are singularities of the transition amplitude on the second Riemann sheet attached to the *physical* boundary of the physical sheet. If they are close enough to the boundary of the physical sheet they produce characteristic variations in the transition amplitude. In our case, the distance onto the second sheet is proportional to Γ , and the singularity is logarithmic. However, since $\Phi(s')$ is also proportional to Γ [through $f_0^*(s')$], the effect of the branch point will be greatest for Γ neither too large nor too small. We will investigate the effect of changing Γ quantitatively in Sec. IV.

We observe that the branch point $s_{-}(s_0)$ moves as M is changed. The range of collision energies M for which $s_{-}(s_0)$ is in the lower half-plane is

$$s_0^{1/2} + \mu < M < \left[\frac{(s_0 + m\mu)(m+\mu) - \mu^3}{m} \right]^{1/2}. \quad (3.9)$$

As M increases to the threshold for resonance production, $s_0^{1/2} + \mu$, the branch point at $s_{-}(s_0)$ approaches $M\mu + (Mm^2 - \mu^3)/(M - \mu)$ from the lower half plane. As M continues to increase, $s_{-}(s_0)$ moves towards threshold just below the s axis, and it curves around the threshold into the upper half plane when $M = [(s_0 + m\mu)(m+\mu) - \mu^3/m]^{1/2}$.¹⁰ If $m \gg \mu$, these equations show that M must lie in a narrow interval, while $s_{-}(s_0)$ is close to threshold. For instance, for pion production by pions, $m = 0.94$ BeV, $\mu = 0.14$ BeV, $s_0^{1/2} = 1.23$ BeV for the (3,3) resonance. Then 1.3700 BeV $< M < 1.3735$ BeV and 1.17 (BeV)² $< s_{-}(s_0) < 1.20$ (BeV)², while the physical region extends to about 1.51 (BeV)².

Now consider the alternative of pion production by nucleons, $m = 0.14$ BeV, $\mu = 0.94$ BeV, $s_0^{1/2} = 1.23$ BeV. Now $\mu \gg m$, and $2.17 < M < 2.61$ BeV. This is an interval of 440 MeV for M , as compared with 3.5 MeV before. At the same time, 1.17 (BeV)² $< s_{-}(s_0) < 1.40$ (BeV)². Now the branch point occurs as much as halfway from the threshold to the (3,3) resonance, and it is present

¹⁰ When M is just above $s_0^{1/2} + \mu$, the derivative in (3.8) is infinite, and the location $\bar{s}_{-}(s_0)$ must be replaced by the more accurate approximation $s_{-}(s_0) - iC_N(s_0)/2s_0$. For narrow resonances, the qualitative description of the motion of the branch point is still correct.

for bombarding nucleon kinetic energies between 0.725 and 1.74 BeV. An optimum energy for observing the branch point might be ~ 800 MeV. At this energy $s_-(s_0)$ has come close to the real axis, but not yet too close to threshold.

Now let us examine the causes of our conjectured "anomaly" at $s_-(s_0)$. We want to obtain a simple physical explanation for the logarithmic singularity which emerges in the once iterated approximation to $T_0(s)$. In Fig. 6 we picture the final-state interaction in momentum space. We are in the rest system of an isobar formed by m and one of the μ 's; the other μ is in flight along the z axis. When the isobar decays, m comes off at an angle θ with respect to the fleeing μ given by

$$\cos\theta = R(s_0, s) / [U(s_0)]^{1/2}, \quad (3.10)$$

where s is the energy of the system composed of m and the fleeing μ in their center of mass. In order that m interact with the fleeing μ after the isobar decays, we naively require that $\cos\theta = +1$. In Fig. 4, if we identify s' and s_0 , this means that arcs (ab) and (da) give s in terms of s_0 for an interaction between m and the fleeing μ . Nowhere else in the quadrant $(m+\mu)^2 < s, s' < (M-\mu)^2$ is $\cos\theta = +1$.

There is a further requirement. In the Lorentz frame of Fig. 6, the velocity of the emerging m must be greater than the velocity of the fleeing μ . This requirement leads to the restriction on s_0

$$-m\mu + \frac{M^2 m + \mu^3}{m + \mu} < s_0 < (M - \mu)^2. \quad (3.11)$$

We conclude that the m and the fleeing μ will rescatter at energy $s_-(s_0)$ when (3.11) is satisfied; that is, when the branch point of $W(s)$ is in the lower half s plane.

This crude classical argument carries no weight in itself, but in retrospect it provides an appealing interpretation of the branch point we have found, and the structure the branch point induces in the KT amplitude. It also sheds some light on a question which survives from the earliest days of resonance physics. When resonance bands cross in the physical region, an augmentation of the resonance is observed at the intersection of the bands. The question arises of whether this augmentation is due solely to symmetrization of the transition amplitude, or is partly due to dynamical effects. In our terms the question is whether $T_0(s)$ is additionally augmented at s_0 by the presence of the overlapping resonance. Mathematically, the answer is that $T_0(s)$ has no such augmentation within the framework of the KT representation and our approximation to its solution. In addition, the success of the classical argument suggests that it may be generally indicative, even though it ignores the quantum-mechanical nature of the process. Insofar as the argument is valid, it shows that one is looking in the wrong place in expecting an augmentation at s_0 . Angle and velocity requirements

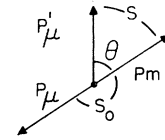


FIG. 6. Final-state interaction in momentum space.

place the most striking contribution from the overlapping resonance at $s_-(s_0)$. Of course, the KT representation cannot give anything as strong as a multiplicative augmentation where the bands cross. The point we stress is that our classical argument contradicts any model which postulates a multiplicative augmentation where bands cross.

We can also discuss singularities which arise in further iterative approximations to $T_0(s)$. These will be analogous to the logarithmic singularity which appears at $\bar{s}_-(s_0)$ in $T_{0,1}(s)$. We are interested only in singularities which appear in the lower half s plane, because only these can produce observable bumps in T . We first state our conclusions, and then give arguments. We will find that higher iterative approximations have singularities in addition to those below s_0 and $s_-(s_0)$ only if M is such that $s_-(s_0)$ is in the lower half plane; that is, M is in the range (3.9). At each iteration we get at most one new singularity in the lower half plane, and at each step the new singularity lies closer to threshold than any singularity found previously. Thus, as we have seen, $s_-(s_0) < s_0$, and all further singularities appearing in $T_{0,2}(s), T_{0,3}(s), \dots$ will be closer to threshold than $s_-(s_0)$. Each singularity is "weaker" than any singularity found previously. For instance, there is a pole in $T_{0,0}(s)$ at s_0 , and a new logarithmic singularity in $T_{0,1}(s)$ at $s_-(s_0)$. The further singularity of $T_{0,2}(s)$ is at $s_-(s_-(s_0))$ (if it exists), and is a finite singularity. For $m \neq 0$ only a finite number of singularities appear. After some step in the iteration procedure we find only singularities which appeared before. For pion production by pions there are at most two singularities, the pole at s_0 , and the logarithmic branch point which appears for M in range (3.9). For pion production by nucleons, there are at most three singularities—the two we have found plus a new one $T_{0,2}(s)$ at $s_-(s_-(s_0))$, which is a finite singularity. As $m/\mu \rightarrow 0$ the maximum number of singularities increases to infinity, but as we can see, m/μ must be quite small before the number of singularities is large. Finally, we note that while (3.9) gives the range of M for which the logarithmic singularity is present, the upper limits of the ranges for which the weaker singularities are present are successively closer and closer to $s_0^{1/2} + \mu$. What this means is that as M increases above threshold for production of a resonance, the singularities move one after another around the threshold into the upper half s plane. The weakest and lowest lying singularity goes first, followed by all the rest, with $s_-(s_0)$ moving to the upper half plane last.

Now for the arguments. We go back to Fig. 5, and observe that the same diagram is obtained if we

interchange the roles of s and s' . At the same time we must interchange the point labels a and d , and b and c so that Figs. 4 and 5 observe consistent notation. Then Fig. 5 displays the trajectories of the logarithmic branch points of $G(s, s', M^2 + i\delta)$ in the complex s' plane as s increases from $(m + \mu)^2$ to ∞ . We see that curves A and B of Fig. 4 map singularities of $T_{0,i}(s')$ into (pinch) singularities of $T_{0,i+1}(s)$. However, arcs (ab) , (bc) and (ad) of Fig. 4 locate new singularities in $T_{0,i+1}(s)$ only from singularities in $T_{0,i}(s')$ slightly below the real s' axis, since a pinch of the integration contour must occur. Conversely, arc (cd) maps singularities in $T_{0,i+1}(s)$ from singularities in $T_{0,i}(s')$ above the real s' axis. The location of the new singularities of $T_{0,i+1}(s)$ can be found by examining the derivatives $\partial s_{\pm}(s')/\partial s'$ in Fig. 4. One sees that arcs (bc) and (cd) map singularities of $T_{0,i}(s')$ in the lower half plane into singularities of $T_{0,i+1}(s)$ in the upper half plane. Arc (ad) maps upper half plane to upper half plane, and arc (ab) maps lower half plane to lower half plane. Hence, only arc (ab) is functional in locating physically significant new singularities at each step of iteration. We need not keep track of singularities in the upper half plane; they do not give rise to singularities in the lower half plane in any subsequent iteration.

From examination of Fig. 4 one sees that each new singularity, s_n , lies at a lower energy than its predecessors. The progressive weakening of the singularities is due to the logarithmic character of G . For instance, the new singularity of $T_{0,2}(s)$ is finite because

$$\int_0^{\infty} (\ln|x|)^2 dx < \infty. \tag{3.12}$$

Clearly, s_0 must lie in range (3.11) for even $s_-(s_0)$ to be a singularity; then $s_-(s_0)$ must lie in range (3.11) for $s_-(s_-(s_0))$ to be a singularity, and so on. In general, the new singularity of $T_{0,n}(s)$ is at

$$s_n = s_{-n}(s_0), \text{ if } s_{n-1} > -m\mu + (M^2m + \mu^3)/(m + \mu). \tag{3.13}$$

At some step s_{n-1} does not satisfy the inequality (3.13), and we find no further singularities. The only alternative is that there be a point of accumulation of the s_n above $-m\mu + (M^2m + \mu^3)/(m + \mu)$. Since the s_n accumulate at threshold if there is an infinite number of them, we must have $-m\mu + (M^2m + \mu^3)/(m + \mu) = (m + \mu)^2$, or $m = 0$, for there to be an infinite number of singularities. This can be understood from our

classical argument. A singularity s_n corresponds to the formation of at least $(n + 1)$ successive isobars prior to the exit of the final-state particles from the volume of interaction. As n increases it becomes more and more difficult to satisfy the velocity requirement. Only if $m = 0$ —that is, only if the “chasing” particle m moves with the speed of light—can we satisfy the velocity requirement for any n .

The maximum number of singularities in practical cases is easily calculated. As M increases above $s_0^{1/2} + \mu$, point a in Fig. 4 moves to the right. On the other hand, $\partial s_-(s_0)/\partial M < 0$. Thus, the greatest number of singularities is present when $M = s_0^{1/2} + \mu$; that is, at threshold for resonance production. $s_-(s_0)$ is then always a logarithmic singularity of $T_{0,1}(s)$. For $s_-(s_0)$ to be a singularity of $T_{0,2}(s)$ we require $s_-(s_0) > -m\mu + (M^2m + \mu^3)/(m + \mu)$, or

$$-m\mu + \frac{M^2m + \mu^3}{m + \mu} < M\mu + \frac{Mm^2 - \mu^3}{M - \mu} (M = s_0^{1/2} + \mu), \tag{3.14}$$

or

$$s_0^{1/2} + \mu < \mu^2/m.$$

Since $s_0^{1/2} > m + \mu$, (3.14) can be satisfied only if

$$m/\mu < 2^{1/2} - 1. \tag{3.15}$$

Equation (3.15) is not satisfied for pion production by pions, so $T_{0,1}(s)$ contains all physically significant singularities of $T_0(s)$ found in any order of iteration. On the other hand, (3.15) is satisfied for pion production by nucleons, and $T_{0,2}(s)$ has a singularity at $s_-(s_0)$ for a small range of M . But $s_-(s_0) = 1.22 \text{ (BeV)}^2$, while $-m\mu + (M^2m + \mu^3)/(m + \mu) = 1.25 \text{ (BeV)}^2$ for $M = s_0^{1/2} + \mu$. Thus, $T_{0,3}(s)$ has no new singularities for any M . In general, our discussion shows that only refinements emerge from a continuation of the iteration procedure. No striking structure of T_0 is present in the exact solution of (2.11) which is not already present in $T_{0,1}$. To be sure, the overlapping resonance produces a smooth background augmentation to T which may change as we improve the solution of (2.11). But this smooth background is relatively uninteresting.

IV. EVALUATION OF THE TRANSITION AMPLITUDE

From (2.3), (2.10), and (2.19), the successive approximations to $T_0(s)$ produce a sequence of approximations to T .

$$T_i(s_a, s_b, s_c) = L_i(s_b) + L_i(s_c), \quad L_i(s) = \frac{1}{\pi} \int_{(m+\mu)^2}^{\infty} \frac{ds' T_{0,i}(s') f_0^*(s')}{s' - s - i\epsilon},$$

$$L_1(s) = L_0(s) + \Gamma F(s), \quad L_0(s) = T_0(s) = \frac{1}{s - s_0 + i\Gamma[s - (m + \mu)^2]^{1/2}}, \tag{4.1}$$

$$F(s) = -\frac{1}{\pi} \int_{(m+\mu)^2}^{\infty} \frac{ds' s' [s' - (m + \mu)^2]^{1/2}}{[U(s')]^{1/2} [s' - s - i\epsilon] \{s' - s_0 - i\Gamma[s' - (m + \mu)^2]^{1/2}\}} \ln \frac{R(s', s_0) + [U(s)]^{1/2} + iC_N(s')}{R(s', s_0) - [U(s)]^{1/2} + iC_D(s')}.$$

The integral $F(s)$ cannot be obtained in terms of elementary functions. However, we can extract the information we want by a simple approximation. Let $k' = [s' - (m + \mu)^2]^{1/2}$. Then

$$F(s) = -\frac{2}{\pi} \int_0^\infty \frac{dk' k' (k'^2 + k_1^2)}{[V(k'^2)]^{1/2} [k'^2 - k_0^2] [k'^2 - k^2 - i\epsilon]} \ln \frac{R(k'^2 + k_1^2, s_0) + k' [V(k'^2)]^{1/2} + i\bar{C}(k')}{R(k'^2 + k_1^2, s_0) - k' [V(k'^2)]^{1/2} + i\bar{C}(-k')}, \quad (4.2)$$

where

$$\begin{aligned} k_1 &= m + \mu, \\ k_0 &= \{s_0 - i\Gamma[s_0 - (m + \mu)^2]^{1/2}\}^{1/2}, \\ k &= \{s - (m + \mu)^2\}^{1/2}, \\ k' [V(k'^2)]^{1/2} &= [U(k'^2 + k_1^2)]^{1/2}, \\ \bar{C}(k') &= C_N(k'^2 + k_1^2), \\ \bar{C}(-k') &= C_D(k'^2 + k_1^2); \end{aligned}$$

and we have made the numerically unimportant approximation of taking k_0 to be independent of k . The integrand of (4.2) is an even function of k , so we may extend the lower limit of the integration to $-\infty$ and divide by 2.

If we are content to obtain only the variation of $F(s)$ near $s_-(s_0)$, we may replace the argument of the logarithm in (4.2) by a function which is a good approximation near $k_-(s_0) = [s_-(s_0) - (m + \mu)^2]^{1/2}$, and hence near $k=0$, but which may be inaccurate farther away. Thus, we want a function which has zeros of the numerator and denominator at the proper points and goes to 1 at $k=0$. Such a function is

$$\begin{aligned} &\frac{k^2 - B + Ck + i\gamma D}{k^2 - B - Ck + i\gamma D}, \\ A &= M^2 + m^2 + 2(\mu^2 - s_0 - s_-(s_0)), \\ B &= k_-^2(s_0) + Ck_-(s_0), \\ [V(k_-^2(s_0))]^{1/2} &= AC, \\ \bar{C}(k_-(s_0)) &= \gamma AD, \\ R(k^2 + k_1^2, s_0) &= A(k^2 - B). \end{aligned} \quad (4.3)$$

Here, A must be large compared with $k_-^2(s_0)$ for the approximation to R to be good. In the example presented below this criterion is satisfied. We insert (4.3) into (4.2), at the same time removing the factor $[V(k'^2)]^{1/2}$, which varies slowly near $k_-(s_0)$, from under the integral sign. Then

$$F(s) = H(s) - \frac{1}{\pi AC} \int_{-\infty}^\infty \frac{dk' k' (k'^2 + k_1^2)}{(k'^2 - k_0^2)(k'^2 - k^2 - i\epsilon)} \times \ln \frac{k'^2 - B + Ck' + i\gamma D}{k'^2 - B - Ck' + i\gamma D}, \quad (4.4)$$

where $H(s)$ varies slowly with s and Γ (or γ) near $s = s_-(s_0)$. The remaining integral, which contains the variation of interest, may be evaluated by factoring

the argument of the logarithm and expressing the integral as a sum of two integrals, one with a cut only in the upper half plane, and the other with a cut only in the lower half plane. These integrals may be worked out by closing the contour in the half plane where only poles are present.

$$F(s) = H(s) - \frac{2i}{AC(s - s_0 - i\gamma s_0^{1/2})} \times \left\{ s \ln \frac{[s - (m + \mu)^2]^{1/2} - k_1}{[s - (m + \mu)^2]^{1/2} - k_2} + (s_0 + i\gamma s_0^{1/2}) \times \ln \frac{[s_0 - (m + \mu)^2 + i\gamma s_0^{1/2}]^{1/2} - k_1}{[s_0 - (m + \mu)^2 + i\gamma s_0^{1/2}]^{1/2} - k_2} \right\}, \quad (4.5)$$

$$\begin{aligned} k_1 &= -\frac{C}{2} + \frac{1}{2}[C^2 + 4B - 4i\gamma D]^{1/2}, \\ k_2 &= C + k_1. \end{aligned}$$

In this expression the arguments of the logarithms are negative.

Now let us look at an example. We study the reaction $N + N \rightarrow N + N + \pi$, where as always our particles and “(3,3)” resonance are spinless. We take $M = 2.25$ BeV, which corresponds to a bombarding kinetic energy of 820 MeV; $m = 0.14$ BeV, $\mu = 0.94$ BeV, $s_0 = 1.518$ (BeV)², and $s_-(s_0) = 1.23$ (BeV)². For narrow resonances, $\text{Re}L_0(s) \gg \text{Im}L_0(s)$ near $s_-(s_0)$, and likewise the variation of $F(s)$ occurs mostly in its real part. [The argument of the logarithm in (4.5) changes by π as the branch point is passed.] Thus, for small γ

$$\begin{aligned} \text{Re}L_1(s) &\approx \text{Re}\gamma \left[\frac{s_0}{s_0 - (m + \mu)^2} \right]^{1/2} H(s) \\ &+ \frac{1}{s - s_0} \left[1 + 12\gamma + 3.2\gamma \right. \\ &\quad \left. \times \tan^{-1} \frac{0.75\gamma}{[s - (m + \mu)^2]^{1/2} - 0.266} \right], \quad (4.6) \\ \text{Im}L_1(s) &\approx \text{Im}\gamma \left[\frac{s_0}{s_0 - (m + \mu)^2} \right]^{1/2} H(s), \end{aligned}$$

where the arctangent is negative. We have computed $\{s_0/[s_0 - (m + \mu)^2]\}^{1/2} H(s_-(s_0))$ by hand; it is $33 - i26$. When the factor $(s - s_0)^{-1}$ of the variation is taken into

account, the contribution of $H(s)$ to $F(s)$ in (4.4) is of the same order of magnitude as the integral contributing the variation. Thus, we obtain Table I, which gives $\text{Re}L_1(s)$ for two resonance widths.

We observe from Table I that the effect of the negative step in the arctangent in (4.6) is largely masked by the rising factor $(s-s_0)^{-1}$. We might hope that by increasing γ we could overcome this cancellation. We observe that this is happening as we increase γ from 25 to 50 MeV. Of course, we are getting away from the narrow resonance limit we have assumed, but apart from this there is a fundamental difficulty in trying to obtain an observable effect by increasing γ . The difficulty is that $\text{Im}L_0(s)$, which we can ignore for small γ , rises like $[s-(m+\mu)^2]^{1/2}$ from threshold. When γ gets much above 50 MeV this rapidly rising imaginary part offsets the falling real part, and $|T(s_a, s_b, s_c)|^2$ still rises for fixed s_c as s_b passes $s_-(s_0)$. We note that this cancellation arises because $f_0(s)$ is unitary and rises like $[s-(m+\mu)^2]^{1/2}$ at threshold.

There are two other possibilities we can think of for making the branch point observable. One is to increase s_0 so that $(s-s_0)^{-1}$ is flatter near threshold. Then we might get a variation for small γ . To do this we must also increase M , so that $s_-(s_0)$ is in the lower half plane. But this increases the factor AC in (4.5). As a result, in order that $\text{Re}L_1(s)$ fall significantly as we pass $s_-(s_0)$ we must again increase γ to the point that the rise in $\text{Im}L_1(s)$ masks the effect.

Finally, one might try to make the scattering length of $f(s)$ near threshold independent of the location and width of the resonance. That is, one might take for $f_0(s)$ the unitary parametrization

$$f(s) = -\frac{A[s-(m+\mu)^2]^{1/2}}{1+iA[s-(m+\mu)^2]^{1/2}} - \left\{ \frac{\Gamma[s-(m+\mu)^2]^{1/2}}{s-s_0+i\Gamma[s-(m+\mu)^2]^{1/2}} \right\} \times \left\{ \frac{1-iA[s-(m+\mu)^2]^{1/2}}{1+iA[s-(m+\mu)^2]^{1/2}} \right\}. \quad (4.7)$$

When $L_1(s)$ is computed using this scattering amplitude, the results are again disappointing. For small scattering length A the variation in $\text{Re}L_1(s)$ is small, while for large A the rise in $\text{Im}L_1(s)$ masks the variation.

We conclude that it is unlikely that we can detect a variation in T due to the branch point of $T_{0,1}(s)$. The same conclusion can be drawn, *mutatis mutandis*,

$$u(s) = -\frac{[s-(m+\mu)^2]}{2\pi i} \int_{-\infty}^{\infty} \frac{dk'}{k'(k'^2-k^2)} \ln(k'-[k_0^2-\Gamma^2/4]^{1/2}+i\Gamma)(k'+[k_0^2-\Gamma^2/4]^{1/2}+i\Gamma) + \frac{[s-(m+\mu)^2]}{2\pi i} \int_{-\infty}^{\infty} \frac{dk'}{k'(k'^2-k^2)} \ln(k'-[k_0^2-\Gamma^2/4]^{1/2}-i\Gamma)(k'+[k_0^2-\Gamma^2/4]^{1/2}-i\Gamma). \quad (A3)$$

TABLE I. Real part of $L_1(s)$ near threshold.

s	$\gamma=0.025$ BeV $\text{Re}L_1(s)$	$\gamma=0.05$ BeV $\text{Re}L_1(s)$
1.17	-2.99	-2.86
1.19	-3.08	-3.03
1.21	-3.31	-3.16
1.23	-3.31	-3.10
1.25	-3.25	-3.01
1.27	-3.49	-3.14
1.29	-3.82	-3.47
	($\text{Im}L_0 = -33$ at $s=s_0$)	($\text{Im}L_0 = -16$ at $s=s_0$)

for the weaker singularity in $T_{0,2}(s)$. These conclusions disagree with Aitchison⁶ because the triangle amplitude which he considers, and which first appears in our L_1 , is swamped by the much larger pole amplitude present in L_0 and L_1 . As we have indicated, the unitarity and threshold behavior of $f_0(s)$ govern the relative strength of these amplitudes near the logarithmic branch point of L_1 .

ACKNOWLEDGMENTS

The author expresses his gratitude to Professor C. Kacser for many helpful discussions. Professor S. B. Treiman suggested this topic and gave essential encouragement and advice as the work progressed.

APPENDIX

We first compute

$$u(s) = -\frac{[s-(m+\mu)^2]}{2\pi i} \int_{(m+\mu)^2}^{\infty} \frac{ds'}{[s'-s-i\epsilon][s'-(m+\mu)^2]} \times \ln \frac{s'-s_0+i\Gamma[s'-(m+\mu)^2]^{1/2}}{s'-s_0-i\Gamma[s'-(m+\mu)^2]^{1/2}}. \quad (A1)$$

Introduce the variables

$$k' = [s'-(m+\mu)^2]^{1/2}, \quad k = [s-(m+\mu)^2+i\epsilon]^{1/2}, \\ k_0 = [s_0-(m+\mu)^2]^{1/2}.$$

$$u(s) = -\frac{[s-(m+\mu)^2]}{\pi i} \int_0^{\infty} \frac{dk'}{k'(k'^2-k^2)} \times \ln \frac{k'^2-k_0^2+i\Gamma k'}{k'^2-k_0^2-i\Gamma k'}. \quad (A2)$$

The integrand of (4.2) is even in k' . We extend the lower limit to $-\infty$ and divide by 2, factor the argument of the logarithm, and split $u(s)$ into two terms.

The first term has a cut only in the lower half k' plane, and the second term has a cut only in the upper half k' plane. They may be evaluated easily, and

$$u(s) = -\ln(s - s_0 + i\Gamma[s - (m + \mu)^2]^{1/2}) - i\pi, \tag{A4}$$

where the argument of the logarithm is $-\pi$ when $s = (m + \mu)^2$.

Next we compute

$$W(s) = \frac{\Gamma s}{\pi[U(s)]^{1/2}} \int_{(m+\mu)^2}^{\infty} \frac{ds' [s' - (m + \mu)^2]^{1/2}}{(s' - s_0)^2 + \Gamma^2 [s' - (m + \mu)^2]} \ln \frac{R(s, s') + [U(s)]^{1/2}}{R(s, s') - [U(s)]^{1/2}}. \tag{A5}$$

Again, let $k' = [s' - (m + \mu)^2]$, $k_0 = [s_0 - (m + \mu)^2]^{1/2}$, $k_{\pm}(s) = \{R(s, (m + \mu)^2) \pm [U(s)]^{1/2}\}^{1/2}$.

$$W(s) = \frac{2\Gamma s}{\pi[U(s)]^{1/2}} \int_0^{\infty} \frac{dk' k'^2}{(k'^2 - k_0^2) + \Gamma^2 k'^2} \ln \frac{k'^2 - k_+^2(s)}{k'^2 - k_-^2(s)}. \tag{A6}$$

The integrand is again an even function of k' . We factor the denominator and split the integral into two terms.

$$W(s) = \frac{\Gamma s}{\pi[U(s)]^{1/2}} \int_{-\infty}^{\infty} \frac{dk' k'^2}{(k' - k_1)(k' - k_2)(k' - k_1^*)(k' - k_2^*)} \ln \frac{k' - k_+(s)}{k' - k_-(s)} + \frac{\Gamma s}{\pi[U(s)]^{1/2}} \int_{-\infty}^{\infty} \frac{dk' k'^2}{(k' - k_1)(k' - k_2)(k' - k_1^*)(k' - k_2^*)} \ln \frac{k' + k_+(s)}{k' + k_-(s)}, \tag{A7}$$

$$k_{1,2} = \pm [k_0^2 - \Gamma^2/4]^{1/2} + i\Gamma/2.$$

The first integrand in (A7) has a cut only in the upper half plane, while the second integrand has a cut only in the lower half plane. The integrals may be evaluated by closing the contour in the half plane where only poles are present.

$$W(s) = \frac{s}{[U(s)]^{1/2}} \left\{ \ln \frac{R(s, s_0) + [U(s)]^{1/2} + iC_N(s)}{R(s, s_0) - [U(s)]^{1/2} + iC_D(s)} - \frac{i\Gamma}{[k_0^2 - \Gamma^2/4]^{1/2}} \ln \frac{[k_1^* - k_+(s)][k_1 + k_-(s)]}{[k_1^* - k_-(s)][k_1 + k_+(s)]} \right\}, \tag{A8}$$

where

$$C_{N,D}(s) = 2\Gamma s k_{\pm}(s). \tag{A9}$$

When $s = (m + \mu)^2$, $k_+ = k_- > 0$. By following $k_{\pm}(s)$ we find that (3.7) holds. For small Γ we can drop the second term of (A8), which has the same singularities as the first term. Finally, $W(s)$ does not have the singularity which is generally found at $s = -m\mu + (M^2 m + \mu^3)/(m + \mu) + i\delta$ [endpoint singularity of (A6) at $(k=0)$]. This is because the integrand of (A6) is an even function of k .